EUROPEAN JOURNAL OF COMPUTATIONAL MECHANICS, 2018
VOL. 27, NO. 1, 33–57
https://doi.org/10.1080/17797179.2018.1439150

Taylor & Francis
Taylor & Francis Group

MHD forces on double diffusive free convection process along a vertical wavy surface embedded in a doubly stratified fluid-saturated Darcy porous medium under the influence of Soret and Dufour effect

S. V. S. S. N. V. G. Krishna Murthy and Vinay Kumar

Department of Applied Mathematics, Defence Institute of Advanced Technology, Deemed University, Pune, India

ABSTRACT

The objective of this paper is to investigate the combined heat and mass transfer process near a vertical wavy semi-infinite surface embedded in a doubly stratified electrically conducting fluid-saturated Darcy porous medium under the influence of Soret and Dufour effects. The governing coupled non-dimensional partial differential equations are transformed to boundary layer equations using the two point local non-similarity transformation which is obtained by scale analysis. The resulting boundary layer equations are solved numerically by applying the Keller Box finite difference scheme. The heat and mass transfer has been analysed by plotting the Local, Average Nusselt and Sherwood numbers for various values of parameters influencing the model like: M_g (Magnetic field effect), a (amplitude of wavy surface), S_T and S_C (Thermal and Mass Stratification), S_r (Soret number), D_f (Dufour number), Buoyancy ratio (B), Lewis number (Le).

ARTICLE HISTORY
Received 1 February 2017
Accepted 16 January 2018

KEYWORDS
Darcy; porous; Soret & Dufour; stratification; Boundary layer; MHD

Nomenclature

$\bar{a}$	dimensional amplitude of the wavy surface
a	non-dimensional amplitude of the wavy surface
B	buoyancy ratio
C	non-dimensional species concentration
c	dimensional species concentration
c_p	specific heat at constant temperature
c_s	concentration susceptibility
c_w	constant vertical wavy wall concentration
D	mass diffusivity of the porous medium
D_f	Dufour effect number
E	electrical conductivity
f	non-similar stream function

CONTACT S. V. S. S. N. V. G. Krishna Murthy sgkmurthy@gmail.com, skmurthy@diat.ac.in

g	gravitational acceleration
K	permeability of the porous medium
k	thermal conductivity
K_T	thermal diffusion ratio
ℓ	wavelength parameter of the surface waves
Le	Lewis number
m_d	applied magnetic flux
M_g	magnetic field parameter
n	outward unit normal to the surface
Nu	Nusselt number
Ra	Rayleigh number
S_r	Soret effect number
S_C	non-dimensional mass stratification parameter
s_c	dimensional mass stratification parameter
S_T	non-dimensional thermal stratification parameter
s_t	dimensional thermal stratification parameter
Sh	Sherwood number
T	non-dimensional temperature
t	dimensional temperature
T_m	mean fluid temperature
t_w	constant vertical wavy wall temperature
u, v	dimensional velocity components
V	velocity vector
x, y	dimensional Cartesian coordinates
X, Y	non-dimensional Cartesian coordinates

Greek symbols

α	thermal diffusivity
β_c	concentration expansion coefficient $\left(\beta_c = -(1/\rho)(\partial\rho/\partial c)_{P,t}\right)$
β_t	thermal expansion coefficient $\left(\beta_t = -(1/\rho)(\partial\rho/\partial T)_{P,c}\right)$
μ	dynamic viscosity of fluid
ν	kinematic viscosity of fluid
ϕ	phase of the wavy surface
$\overline{\Psi}$	dimensional stream function $\left(u = \partial\overline{\Psi}/\partial y, v = -\partial\overline{\Psi}/\partial x\right)$
Ψ	non-dimensional stream function
ρ	fluid density $\left(= \rho_0[1 - \beta(t - t_\infty) - \beta(c - c_\infty)]\right)$
σ	sinusoidal wavy curve $\left(\sigma(X) = \frac{a}{\pi}\sin(\pi X - \phi)\right)$
ξ, η	transformed coordinate variables

Subscripts

∞ ambient points
c concentration
P pressure
t temperature
w evaluated at wall
x evaluated at point x

1. Introduction

The study (Nield & Bejan, 2006; Vafai, 2015; Vafai & Hadim, 2000) of heat and mass transfer process through natural convection phenomenon within fluid-saturated porous media is an attracting area of research because of its importance in engineering as well as industrial applications such as oil recovery techniques, geophysics, heat storage beds, packed-bed catalytic reactors, thermal insulation engineering. Additionally, the area of heat transfer from irregular surfaces has become the topic of fundamental importance due to occurrences of enhanced heat transfer by surfaces with intentionally placed roughness elements in many heat transfer devices, e.g. flat-plate condensers in refrigerators and flat-plate solar collectors. Furthermore, the analysis of heat and mass transfer process under the influence of applied magnetic field on an electrically conducting fluid-saturated porous medium has been a major topic of research, due to its implementation in industrial and technological applications such as oil extraction, electronic cooling, solar collectors, crystal growth, nanoduct flows, nanomotors, nanogenerators, nanopumps, nanoactuators. On the other hand, it is often encountered that heat flux is generated by not only temperature gradients but also concentration gradients (diffusion-thermo) as well as mass flux is produced by not only concentration gradients but also temperature gradients (thermal-diffusion). The study of such a behaviour of heat and mass transfer is also important because of its theoretical and practical implementations as the flow near wells of oil or gas production, water pumping and liquid waste injection, etc. The influence due to Soret and Dufour effect on heat and mass transfer by natural convection in Newtonian fluid has been found to be significantly considerable so that it cannot be neglected (Tsai & Huang, 2009) because of its utilisation for isotope separation in a mixture between very light molecular weight (H_2, He) and medium molecular weight (H_2, air), etc. Moreover, the MHD fluid flow along the wavy surfaces, having the complexities: thermal and mass stratification of fluid in Darcy porous medium has been the eminent area of interest of researchers and engineers due to its importance in design of fuel tank in both ground and space-based propellant storage systems, Thermal energy storage tanks, Thermocline thermal energy storage system, reservoir, Nuclear tanks, Design of cryogenic engine tanks, Homogeneous charge compression ignition Engines. The detailed study of literature survey is mentioned below.

Bejan and Khair (1985) reported a principal study of the process of double diffusive free convection in the ambient of vertical wall immersed within the fluid-saturated porous medium. Cheng (2000) reported a study of free convective heat and mass transfer phenomenon near vertical wavy surface immersed in a fluid-saturated porous medium incorporating the complex wavy surface to a smooth surface coordinate transformation applied using the local non-similarity method. Then the obtained equations are solved numerically by the cubic spline collocation method. In addition to this study, Cheng (2009) extended to the power-law fluid by considering the thermal and concentration stratification effects too. Elgazery and Elazem (2009) investigated the effects of variable viscosity and thermal conductivity on MHD unsteady natural convection over a vertical wavy surface by applying an implicit marching Chebyshev collocation scheme. Geindreau and Auriault (2002) studied the magnetohydrodynamic flows in porous media and reported the fact that the macroscopic mass is coupled electric currents and exhibit the dependence on the electric field and macroscopic gradient of pressure. Gorla and Chamkha (2011) presented an analysis of free convective boundary layer flow over a non-isothermal vertical surface immersed in the nanofluid-saturated porous medium. Hady, Mohamed, and Mahdy (2006) introduced a study of heat generation ro absorption effects on MHD natural convection flow. The transformed boundary layer equations are solved numerically using Runge–Kutta integration scheme with the shooting technique. Ingham and Pop (2005) have provided a comprehensive study of transport phenomenon in porous media and various complexities. Kabir, Alim, and Andallah (2013) reported the effect of heat generation and viscous dissipation on MHD free convection flow near a vertical wavy surface and solved numerically using the implicit finite difference method. Kumar and Shalini (2004) analysed the Darcy free convection process along a double diffusive, doubly stratified vertical wavy surface embedded in a fluid-saturated porous medium. Molla, Hossain, and Yao (2004) investigated heat generation/absorption in the free convective process along a vertical wavy maintained at a uniform surface temperature and then solved numerically by employing the implicit finite difference method.

Postelnicu (2004) analysed the impact of an externally applied magnetic field on natural convection from the vertical surface in porous media by considering the Soret and Dufour effects then solved numerically using a finite difference method. Roussellet, Niu, Yamaguchi, and Magoulés (2011) reported on natural convection flow of a temperature-sensitive magnetic fluid in a porous media and solved numerically using lattice Boltzmann method. Tak and Lodha (2007) investigated the influence of double stratification on MHD free convection vertical surface embedded in Darcy flow with Soret and Dufour effects. Takhar and Ram (1994) analysed the free and forced convection flow in the presence of a uniform transverse magnetic field as a special case of fluid (water at 4 °C). Tashtoush and Al-Odat (2004) investigated the magnetohydrodynamics of forced

convective fluid flow over a wavy surface with a variable heat flux. Narayana and Sibanda (2010) studied numerically the influence of Soret and Dufour effects on natural convection along a vertical wavy surface in a fluid-saturated Darcy porous medium. Rees and Pop (1994, 1997) studied analytically the influence of longitudinally aligned surface waves on natural convection from vertical surfaces in porous media.

So far the present work: free convective heat and mass transfer process along a semi-infinite vertical wavy surface embedded in a doubly stratified fluid-saturated Darcy porous medium under MHD forces, Soret and Dufour effects has not been reported in the literature. Under these influences, a mathematical model has been developed and it is solved by applying two-point local non-similarity transformation which is obtained using scale analysis. The resulting equations are solved numerically by Keller-box implicit finite difference scheme. To analyse the heat and mass transfer: Local/Average Nusselt (Nu) number and Local/Average Sherwood (Sh) number plots has been presented for the parameters such as amplitude effect (a), magnetic field parameter (M_g), thermal (S_T) and mass (S_C) stratification coefficients, buoyancy ratio (B), Lewis number (Le), Soret (S_r) and Dufour (D_f) numbers.

2. Mathematical formulation and solution methodology

A wavy surface aligned vertically, schematic of physical configuration in Figure 1, is considered immersed in a doubly stratified fluid-saturated porous medium where the system is exposed to magnetic forces of intensity m_d applied transversally to the vertical surface in the horizontal direction. Surface profile of the vertical wavy wall is approximated sinusoidal as specified beneath.

$$y = \sigma(x) = \bar{a}\sin\left(\frac{\pi x}{\ell} - \phi\right) \tag{1}$$

Here, leading edge of the vertical wavy surface is positioned at the origin of the coordinate system and x-axis is measured along it. Furthermore, the vertical wavy wall is sustained at a uniform temperature t_w and uniform mass concentration c_w of some constituent in the fluid. At the spot sufficiently outlying from the vertical surface, the ambient temperature and concentration are assumed at $t_{\infty,x}$ and $c_{\infty,x}$, respectively, where $t_{\infty,x}$ and $c_{\infty,x}$ are expressed as:

$$\begin{aligned} t_{\infty,x} &= t_{\infty,0} + s_t x, s_t = \frac{\mathrm{d}t_{\infty,x}}{\mathrm{d}x} \\ c_{\infty,x} &= c_{\infty,0} + s_c x, s_c = \frac{\mathrm{d}c_{\infty,x}}{\mathrm{d}x} \end{aligned} \tag{2}$$

Considering the below assumptions

- The fluid flow is Darcy, two-dimensional, incompressible, laminar, steady, electrically conducting.

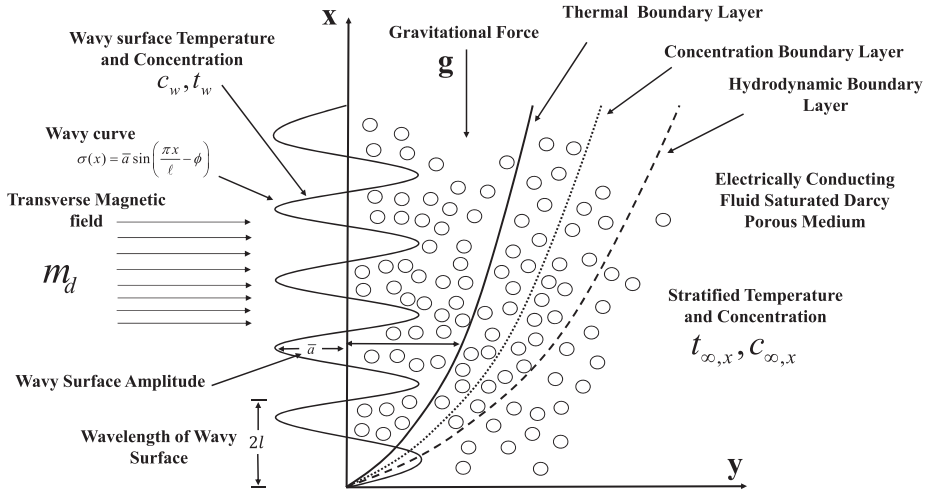

Figure 1. Schematic diagram of the physical model with prescribed boundary conditions and the coordinate system.

- The fluid and solid porous matrix is supposed at local thermal equilibrium all over the domain.
- The medium is considered homogeneous and isotropic.
- The properties of the porous medium and fluid are constants other than the density variations with temperature and concentration where density is formulated mathematically by the Boussinesq approximation $\rho = \rho_0\left[1 - \beta_t\left(t - t_0\right) - \beta_c\left(c - c_0\right)\right]$ where:

$$\beta_t = -\frac{1}{\rho}\left(\frac{\partial \rho}{\partial t}\right)_{P,c}, \qquad \beta_c = -\frac{1}{\rho}\left(\frac{\partial \rho}{\partial c}\right)_{P,t}$$

  the equations governing the heat and mass transfer process in the presence of Soret and Dufour effects for the Darcy flow through a homogeneous porous medium with magnetic field near the vertical wavy surface in terms of dimensional form can be written as follows:
- Continuity equation

$$\frac{\partial u}{\partial x} + \frac{\partial v}{\partial y} = 0 \tag{3}$$

- Momentum equations

$$\frac{\partial p}{\partial x} = -\frac{\mu}{K}\left(1 + \frac{KEm_d^2}{\mu}\right)u - \rho g; \quad \frac{\partial p}{\partial y} = -\frac{\mu}{K}v \tag{4}$$

- Energy (Heat and Concentration respectively) equation

$$u\frac{\partial t}{\partial x} + v\frac{\partial t}{\partial y} = \alpha\left[\frac{\partial^2 t}{\partial x^2} + \frac{\partial^2 t}{\partial y^2}\right] + \frac{DK_T}{c_p c_s}\left[\frac{\partial^2 c}{\partial x^2} + \frac{\partial^2 c}{\partial y^2}\right] \tag{5}$$

$$u\frac{\partial c}{\partial x}+v\frac{\partial c}{\partial y}=D\left[\frac{\partial^2 c}{\partial x^2}+\frac{\partial^2 c}{\partial y^2}\right]+\frac{DK_T}{T_m}\left[\frac{\partial^2 t}{\partial x^2}+\frac{\partial^2 t}{\partial y^2}\right] \tag{6}$$

The appropriate boundary conditions of the problem are

$$\begin{aligned} &v=0, t=t_w, c=c_w, \text{ on } y=\sigma(x)=\bar{a}\sin\left(\frac{\pi x}{l}\right)\\ &u\to 0, t\to t_{\infty,x}, c\to c_{\infty,x} \text{ as } y\to\infty \end{aligned} \tag{7}$$

Permeability K is determined from the widely known correlation proposed by Ergun's relations (Ergun, 1952).

$$K=\frac{d^2\phi^3}{150(1-\varphi)^2)}$$

where d and φ denote the particle diameter and the porosity, respectively. The above Equations (3)–(6) are transformed to the non-dimensional form by introducing the stream function $\left(u=\partial\overline{\Psi}/\partial y, v=-\partial\overline{\Psi}/\partial x\right)$ and considering the non-dimensional variables as mentioned below:

$$\begin{aligned} &X=\frac{x}{\ell},\ Y=\frac{y}{\ell},\ a=\frac{\overline{a}\,\pi}{\ell},\ \Psi=\frac{\overline{\Psi}}{\alpha},\ Le=\frac{\alpha}{D},\ T=\frac{t-t_{\infty,x}}{t_w-t_{\infty,0}},\ C=\frac{c-c_{\infty,x}}{c_w-c_{\infty,0}},\\ &B=\frac{\beta_c\left(c_w-c_{\infty,0}\right)}{\beta_t\left(t_w-t_{\infty,0}\right)}, S_r=\frac{DK_T}{T_m\,\alpha}\left(\frac{t_w-t_{\infty,0}}{c_w-c_{\infty,0}}\right),\ D_f=\frac{DK_T}{c_p\,c_s\,\alpha}\left(\frac{c_w-c_{\infty,0}}{t_w-t_{\infty,0}}\right),\\ &S_T=\frac{\ell}{\left(t_w-t_{\infty,0}\right)}\frac{\mathrm{d}t_{\infty,x}}{\mathrm{d}x},\ S_C=\frac{\ell}{\left(c_w-c_{\infty,0}\right)}\frac{\mathrm{d}c_{\infty,x}}{\mathrm{d}x},\\ &Ra=\frac{K\,g\,\beta_t\ell(t_w-t_{\infty,0})}{\nu\alpha},\ M_g=\frac{KE\,m_d^2}{\mu} \end{aligned} \tag{8}$$

The governing equations in the non-dimensional form are:

$$\left(\frac{\partial^2\Psi}{\partial X^2}+\frac{\partial^2\Psi}{\partial Y^2}\right)+M_g\frac{\partial^2\Psi}{\partial Y^2}=Ra\left(\frac{\partial T}{\partial Y}+B\frac{\partial C}{\partial Y}\right) \tag{9}$$

$$\left[\frac{\partial^2 T}{\partial X^2}+\frac{\partial^2 T}{\partial Y^2}\right]+D_f\left[\frac{\partial^2 C}{\partial X^2}+\frac{\partial^2 C}{\partial Y^2}\right]=\frac{\partial\Psi}{\partial Y}\frac{\partial T}{\partial X}+S_T\frac{\partial\Psi}{\partial Y}-\frac{\partial\Psi}{\partial X}\frac{\partial T}{\partial Y} \tag{10}$$

$$\frac{1}{Le}\left[\frac{\partial^2 C}{\partial X^2}+\frac{\partial^2 C}{\partial Y^2}\right]+S_r\left[\frac{\partial^2 T}{\partial X^2}+\frac{\partial^2 T}{\partial Y^2}\right]=\frac{\partial\Psi}{\partial Y}\frac{\partial C}{\partial X}+S_C\frac{\partial\Psi}{\partial Y}-\frac{\partial\Psi}{\partial X}\frac{\partial C}{\partial Y} \tag{11}$$

The appropriate boundary conditions in non-dimensional form are:

$$\Psi = 0,\ T = 1 - S_T X,\ C = 1 - S_C X \quad \text{on } Y = \sigma(X) = \frac{a}{\pi}\sin(\pi X)$$
$$\frac{\partial \Psi}{\partial Y} \to 0,\ T \to 0,\ C \to 0 \text{ as } Y \to \infty, \tag{12}$$

3. Solution methodology

3.1. Non-similarity transformation

The detailed explanation of the similarity transformation and non-local similarity transformation has been given by the authors Boerner, Quack, and Sparrow (1970), Yu and Sparrow (1971). Non-similarity in the boundary layer can be caused by various factors like as (i) transverse curvature, (ii) stream-wise alterations in the free-stream velocity, (iii) stream-wise variations of the surface temperature, (iv) surface mass transfer. The problems having boundary layer equations which contain non-similar terms don't admit the similarity solutions. The local-similarity method has a drawback that it doesn't retain the non-similar terms of boundary layer equations so that the obtained results are with uncertain accuracy. To overcome this issue, the non-similarity transformation is employed so that accuracy of results is maintained. In the present study, the local non-similarity approach has been applied.

At this juncture, the Rayleigh number is assumed so large that natural convection can take place with boundary layer which has the cross-stream width significantly less than the ($O(1)$) amplitude of the surface waves. On this account, a new set of variables is defined by deducing the influence of surface waves. Therefore, using the scale analysis we attain the variable transformation (Rees & Pop, 1994) as

$$\xi = X,\ Y = \xi^{1/2} Ra^{-1/2}\,\eta,\ + \sigma(X),$$
$$\Psi = Ra^{1/2}\,\xi^{1/2} f(\xi, \eta). \tag{13}$$

By substituting the transformation (13) into Equations (9)–(11) and in the limiting case $Ra \to \infty$, we obtain following transformed boundary layer equations:

$$\left(1 + \sigma_\xi^2\right)\frac{\partial^2 f}{\partial \eta^2} + M_g \frac{\partial^2 f}{\partial \eta^2} = \frac{\partial T}{\partial \eta} + B\frac{\partial C}{\partial \eta}, \tag{14}$$

$$\left(1 + \sigma_\xi^2\right)\left[\frac{\partial^2 T}{\partial \eta^2} + D_f \frac{\partial^2 C}{\partial \eta^2}\right] + \frac{1}{2} f \frac{\partial T}{\partial \eta} = \xi\left(\frac{\partial f}{\partial \eta}\frac{\partial T}{\partial \xi} + S_T \frac{\partial f}{\partial \eta} - \frac{\partial f}{\partial \xi}\frac{\partial T}{\partial \eta}\right) \tag{15}$$

$$\left(1+\sigma_{\xi}^{2}\right)\left[\frac{\partial^{2}C}{\partial\eta^{2}}+Le\,S_{r}\frac{\partial^{2}T}{\partial\eta^{2}}\right]+\frac{Le}{2}f\frac{\partial C}{\partial\eta}=\xi\,Le\left(\frac{\partial f}{\partial\eta}\frac{\partial C}{\partial\xi}+S_{C}\frac{\partial f}{\partial\eta}-\frac{\partial f}{\partial\xi}\frac{\partial C}{\partial\eta}\right) \tag{16}$$

with the boundary conditions:

$$\begin{aligned} &f=0,\ T=1-S_{T}\,\xi,\ C=1-S_{C}\,\xi \text{ on } \eta=0,\\ &\frac{\partial f}{\partial\eta}\to 0, T\to 0,\ C\to 0 \text{ as } \eta\to\infty. \end{aligned} \tag{17}$$

The non-similar boundary layer Equations (14)–(16) together with boundary conditions (17) are obtained using two-point local non-similarity method.

3.2. Keller Box finite difference method

The Keller Box Method (KBM) developed by Isaacson and Keller (1994), Keller and Cebeci (1971), can be specially derived for boundary layer problems for the systems of ordinary differential equations. The fundamental equations in the form of first-order derivative, are approximated using the central difference scheme at the midpoint of the unit cell of mesh grid sections (rectangles). Most attractive feature of Keller Box method is that it is more accurate and yields the solutions of second-order accuracy even in the case of non-uniformly distributed mesh grids.

Therefore, the Keller Box implicit finite difference scheme has been chosen to solve the resulting coupled non-linear boundary layer partial differential Equations (14)–(16) subjected to the boundary conditions (17) . The non-similar boundary layer Equations (14)–(16) are converted into system of first-order differential equations as follows:

$$\left(1+\sigma_{\xi}^{2}+M_{g}\right)\frac{\partial f}{\partial\eta}=T+BC, \tag{18}$$

$$u=\frac{\partial T}{\partial\eta} \tag{19}$$

$$\left(1+\sigma_{\xi}^{2}\right)\left[\frac{\partial u}{\partial\eta}+D_{f}\frac{\partial v}{\partial\eta}\right]+\frac{1}{2}f\,u=\xi\,\left(\frac{\partial f}{\partial\eta}\frac{\partial T}{\partial\xi}+S_{T}\frac{\partial f}{\partial\eta}-\frac{\partial f}{\partial\xi}\frac{\partial T}{\partial\eta}\right) \tag{20}$$

$$v=\frac{\partial C}{\partial\eta} \tag{21}$$

$$\left(1+\sigma_{\xi}^{2}\right)\left[\frac{\partial v}{\partial\eta}+Le\,S_{r}\frac{\partial u}{\partial\eta}\right]+\frac{Le}{2}f\,v=\xi\,Le\left(\frac{\partial f}{\partial\eta}\frac{\partial C}{\partial\xi}+S_{C}\frac{\partial f}{\partial\eta}-\frac{\partial f}{\partial\xi}\frac{\partial C}{\partial\eta}\right) \tag{22}$$

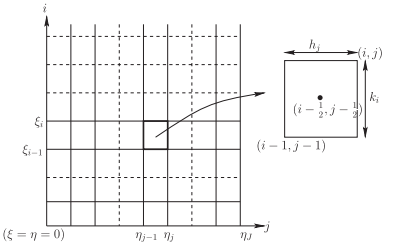

with the boundary conditions:

$$f = 0,\ T = 1 - S_T\,\xi,\ C = 1 - S_C\,\xi \text{ on } \eta = 0,$$
$$\frac{\partial f}{\partial \eta} \to 0, T \to 0,\ C \to 0 \text{ as } \eta \to \infty. \tag{23}$$

We place an arbitrary rectangular net of points (ξ_i, η_j) on $\xi \geq 0, 0 \leq \eta \leq \eta_\infty$ as:

$$\begin{aligned} &(a)\ \ \xi_0 = 0 : \xi_i = \xi_{i-1} + k_i, i = 1, 2, 3, \ldots; \\ &(b)\ \ \eta_0 = 0 : \eta_j = \eta_{j-1} + h_j, j = 1, 2, 3, \ldots, \\ &\text{where } \eta_j = \eta_\infty \end{aligned} \tag{24}$$

The derivatives in Equations (18–22) are approximated by employing central differences at $(\xi_{n-\frac{1}{2}}, \eta_{j-\frac{1}{2}})$ the mid points of mesh segments.

In general, when solution is known at $\xi = \xi_{i-1}$, we proceed to find the solution along the line $\xi = \xi_i$. At each fixed ξ-level, the resulting non-linear algebraic system contains $(5J + 5)$ unknowns, which are computed by means of Newton's method. Iterates are denoted by $\left\{f_j^{(k)}, u_j^{(k)}, T_j^{(k)}, v_j^{(k)}, C_j^{(k)}\right\}$ where k denotes the iteration level. Here, we have removed subscript i for the sake of simplicity. We determine the next approximation at $(k + 1)$ level as:

$$\begin{aligned} &f_j^{(k+1)} = f_j^{(k)} + \delta f_j^{(k)}, \quad u_j^{(k+1)} = u_j^{(k)} + \delta u_j^{(k)}, \quad T_j^{(k+1)} = T_j^{(k)} + \delta T_j^{(k)}, \\ &v_j^{(k+1)} = v_j^{(k)} + \delta v_j^{(k)}, \quad C_j^{(k+1)} = C_j^{(k)} + \delta C_j^{(k)} \end{aligned} \tag{25}$$

Inserting these equations in place of $\left\{f_j, u_j, T_j, v_j, C_j\right\}$ in Equation (25) and dropping the quadratic terms in $\left\{\delta f_j^{(k)}, \delta u_j^{(k)}, \delta T_j^{(k)}, \delta v_j^{(k)}, \delta C_j^{(k)}\right\}$, the resulting linear system of equations can be written in vector matrix form as follows:

$$R_j^{(k)} \delta_j^{(k)} - L_j^{(k)} \delta_{j-1}^{(k)} = r_j^{(k)},\ 1 \leq j \leq J, \text{ for each fixed } i, \tag{26}$$

where

$$\begin{aligned} \delta_j^{(k)} &= \left(\delta f_j^{(k)}, \delta T_j^{(k)}, \delta C_j^{(k)}, \delta u_j^{(k)}, \delta v_j^{(k)}\right)^T, \\ \delta_{j-1}^{(k)} &= \left(\delta f_{j-1}^{(k)}, \delta T_{j-1}^{(k)}, \delta C_{j-1}^{(k)}, \delta u_{j-1}^{(k)}, \delta v_{j-1}^{(k)}\right)^T, \quad 1 \leq j \leq J. \end{aligned} \tag{27}$$

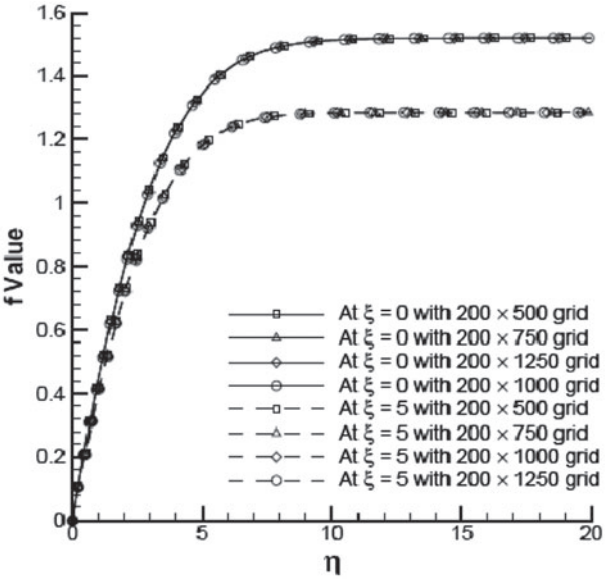

Figure 2. Grid validation tests for various grids at $\xi = 0$, $B = 2$, $Le = 1$, $S_T = 0.05$, $S_C = 0.025$, $a = 0.0$ by comparing results with Bejan and Khair (1985).

The system of coefficient matrices (26) is solved by Newton's method using an efficient block-tridiagonal factorization technique. Convergence is ensured at each fixed ξ, by repeating iteration process to obtain an accuracy of 10^{-10}, using double precision arithmetic throughout. Maximum η-length (η_∞) is chosen as 20 as it is found to lie well outside the boundary layer. A uniform step size of 0.05 is used in ξ-direction, $0 \leq \xi \leq 10$ and a non-uniform grid of 500 points is used in η-direction, $0 \leq \eta \leq 20$, with more points concentrated towards $\eta = 0$. In Figure 2, f-values are shown for different grids at $\xi = 0, 5$. The computational grid of size 200×500 is found to be more than adequate for carrying out the detailed simulations.

3.3. Nusselt number and Sherwood number

Here, Local and Average Nusselt numbers at a vertical distance ξ are Given, respectively by:

$$\frac{Nu_\xi}{Ra\,\xi^{1/2}} = -T'(\xi,0)\left(1+\sigma_\xi^2\right)^{\frac{1}{2}}, \quad \frac{Nu_m}{Ra^{1/2}} = -\xi\frac{\int_0^\xi \frac{\left(1+\sigma_{\overline{X}}^2\right)T'(\overline{X},0)}{\overline{X}^{1/2}}\mathrm{d}\overline{X}}{\int_0^\xi \left(1+\sigma_{\overline{X}}^2\right)^{1/2}\mathrm{d}\overline{X}}, \tag{28}$$

where prime ($'$) denotes the differentiation with respect to η.

Similarly, Local and Average Sherwood number at a vertical distance ξ are given, respectively as:

$$\frac{Sh_\xi}{Ra\,\xi^{1/2}} = -C'(\xi,0)\left(1+\sigma_\xi^2\right)^{\frac{1}{2}}, \quad \frac{Sh_m}{Ra^{1/2}} = -\xi\frac{\int_0^\xi \frac{\left(1+\sigma_{\overline{X}}^2\right)C'(\overline{X},0)}{\overline{X}^{1/2}}\mathrm{d}\overline{X}}{\int_0^\xi \left(1+\sigma_{\overline{X}}^2\right)^{1/2}\mathrm{d}\overline{X}}. \tag{29}$$

4. Results and discussion

The parameters that influence the double diffusive magnetohydrodynamic (MHD) free convection process along a vertical wavy surface embedded in doubly stratified fluid-saturated porous medium with the Darcian assumptions under the influence of Soret and Dufour effects are as (i) amplitude effect (a) (ii) magnetic field parameter (M_g) (iii) thermal (S_T) and mass (S_C) stratification coefficients (iv) buoyancy ratio (B) (v) Lewis number (Le) (vi) Soret (S_r) and Dufour (D_f) number. First, we validate our code (Keller Box Formulation) by comparing the obtained Local Nusselt number and Sherwood number values with the similarity solution values of Bejan and Khair (1985) and Cheng (2000) in case of $a = 0$ (flat surface) at $\xi = 0$ for various B and Le and also validate the code with Mahdy (2009) for Local Nusselt number values for variation of a (wavy surface) at $\xi = 1$. Tables 1 and 2 show that the obtained results are in excellent agreement with those reported in Bejan and Khair (1985), Cheng (2000) and Mahdy (2009). Numerical computations have been carried out to investigate the influence of varying parameters on heat and mass transfer process with Soret and Dufour effects for Darcy flow model. Obtained results with the detailed discussion are as follows:

4.1. Influence of amplitude (a) on heat and mass transfer process

The impact of presence of surface roughness on MHD double diffusive natural convection in Darcy porous medium have been explored for the amplitude of

Table 1. Comparison of Local Nusselt number and Local Sherwood number values from present code (the absence of Thermal (S_T and Concentration (S_C) stratification) for the simple model when $\xi = 0$, $D_f = 0$, $S_r = 0$, for $a = 0$ (flat plate) and the absence of Magnetic field (M_g) are considered with those reported earlier in literature.

		Local Nusselt number $((Ra\,\xi)^{-1/2}Nu_\xi)$			Local Sherwood number $((Ra\,\xi)^{-1/2}Sh_\xi)$		
B	Le	Bejan and Khair (1985)	Cheng (2000)	Present work	Bejan and Khair (1985)	Cheng (2000)	Present work
4	1	0.992	0.9923	0.9921	0.992	0.9923	0.9921
4	4	0.796	0.7976	0.7976	2.055	2.0550	2.0545
4	10	0.681	0.6811	0.6811	3.290	3.2899	3.2887
4	100	0.521	0.5209	0.5209	10.521	10.521	10.5117
1	4	0.559	0.5585	0.5585	1.358	1.3575	1.3572
2	4	0.650	0.6494	0.6495	1.624	1.6243	1.6241
3	4	0.728	0.7278	0.7277	1.852	1.852	1.8520

Table 2. Comparison of Local Nusselt number values from present code in the absence of Thermal (S_T) and Concentration (S_C) stratification for variation of a (wavy surface) at $\xi = 1.0$.

						Local Nusselt number $((Ra\,\xi)^{-1/2}Nu_\xi)$	
a	M_g	Le	B	D_f	S_r	Mahdy (2009)	Present work
0.1	0.0	1.0	1.0	0.050	1.2	0.645661	0.646480
0.2	1.0	1.0	1.0	0.050	1.2	0.437331	0.437436
0.2	1.0	1.0	1.0	0.030	2.0	0.461670	0.451266
0.2	1.0	1.0	1.0	0.037	1.6	0.450309	0.444761

wavy surface parameter $0 \leq a \leq 0.5$ together with the other parameter values fixing at $B = 2$, $Le = 1$, $M_g = 2$, $D_f = S_r = 0.025$, $S_T = S_C = 0.025$. The local, average Nusselt number and local, average Sherwood number plots demonstrating the heat fluxes and mass fluxes along the flat wall are presented in Figure 3(a)–(d). From the Figure 3(a), (c), it can be observed that with raising the amplitude of wavy surface diminish periodically the Local *Nu* and Local *Sh* levels at crest and troughs along the vertical surface. This behaviour of fluid flow is the outcome of an attribute that magnitude of buoyancy forces in ambient a wavy wall is accounted less than or equal to the flat surface which justify the enhanced levels of heat and mass fluxes in comparison with the flat surface. From the Figure 3(b), (d) only marginal variation in Average *Nu* and Avg *Sh* is noted with raising the amplitude of wavy surface. By which it is concluded that the thickness of boundary layers have only insignificant alteration even after raising the wavy nature of the vertical surface.

4.2. Influence of magnetic field parameter M_g on heat and mass transfer process

The affect of applied magnetic field on heat and mass transfer process in doubly stratified Darcy porous medium with presence of Soret and Dufour effect have been analysed by Local, Average *Nu* and Local, Average *Sh* plots in Figure 4(a)–(d) for wide range of $0 \leq M_g \leq 100$, and having fixed $a = 0.3$, $Le = 1$, $B = 1$, $S_T = S_C = 0.025$, $D_f = S_r = 0.02$. From Figure 4(a)–(d), it is observed that raising the magnetic field intensity becomes the cause to drop in Local *Nu* and *Sh*, Average *Nu* and *Sh* all along the vertical surface which is clearly evidence of rise in temperature and concentration levels since the applied magnetic forces resist the horizontal velocity component in addition to enhancing the vertical velocity component of the fluid flow. Hence, reason of drop in Local *Nu* and *Sh* is justified here. From Figure 4(a), (c) it is noted that slight increment in magnetic field intensity leads drastic drop in Local *Nu* and Local *Sh* for small values of $0 \leq M_g \leq 2$, whereas it is marginal for large values of $M_g \geq 2$. From Figure 4(a), (c) it is also perceived that with raising the magnetic field parameter value, wavy nature of Local *Nu* and Local *Sh* reduces and for higher values it tends to vanish.

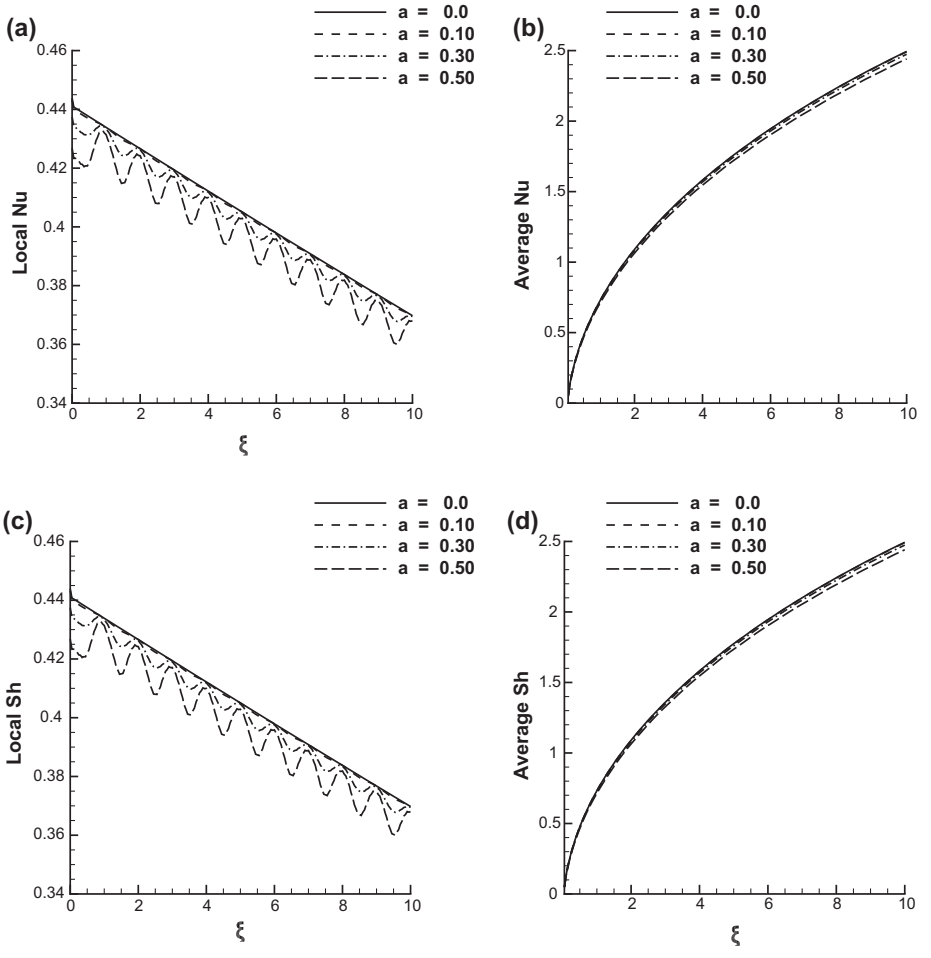

Figure 3. When fixing $Le = 1$, $B = 2$, $Mg = 2$, $S_r = D_f = 0.025$, $S_T = S_C = 0.025$ (a) Local Nu (b) Avg Nu (c) Local Sh (d) Avg Sh plots along the vertical wall for varying *Gr*.

From the Figure 4(a), (c) it is noticed that raising the magnetic field parameter value decrease the impact of thermal and mass stratification along the vertical surface. Such a characteristics of fluid flow is consequence of fact that the increase in M_g boost the temperature and concentration profile by accelerating the flow along the ξ axis or vertical surface and decrease the transverse temperature and concentration gradients. So that over all temperature increase and the decline in temperature gradients diminish stratification along the vertical direction or ξ axis. From Figure 4(b), (d) it is observed that increasing the magnetic field parameter M_g values come out with decrease in the Average *Nu* and Average *Sh*. As a result of which it can be stated that thickness of boundary layer become larger as the magnetic field intensity is given rise. The reason behind this behaviour is the decrement in temperature and concentration gradients (Overall temperature gets same as wall concentration) and growth in velocity profile of fluid as increasing M_g.

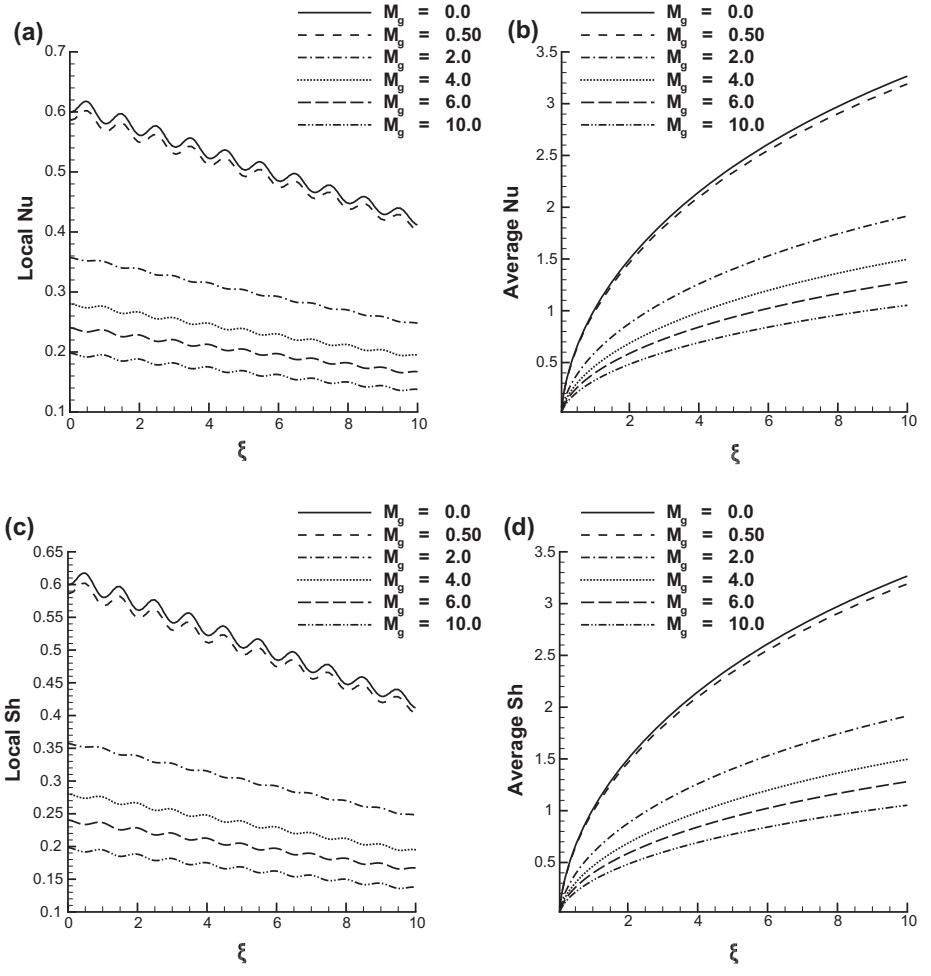

Figure 4. When fixing $a = 0.3, Le = 1, B = 1, S_r = D_f = 0.002, S_T = S_C = 0.025$ (a) Local Nu (b) Avg Nu (c) Local Sh (d) Avg Sh plots along the vertical wall for varying M_g.

4.3. Influence of stratification parameters (S_T) and (S_C) on heat and mass transfer process

To analyse the influence of thermal and concentration stratification on heat and mass transfer process in the presence of magnetic field, Local Nu, Local Sh, Average Nu and Average Sh numbers plots along the surface $0 \leq \xi \leq 10$ are presented for varying thermal stratification parameter ($0 \leq S_T \leq 0.3$) with fixed $S_C = 0.1$ in Figure 5(a)–(d), increasing mass stratification parameter ($0 \leq S_C \leq 0.3$) when fixing $S_T = 0.1$ in Figure 6(a)–(d), varying both thermal and mass stratifications parameter ($0 \leq S_T, S_C \leq 0.3$) in 7 where other parameter are fixed as $a = 0.3, M_g = 2, Le = 1, B = 1, D_f = S_r = 0.025$.

From the Figure 5(a), (c) it is observed that Local *Nu* and Local *Sh* curve are parallel to ξ with certain amount of periodic fluctuation due to wavy nature

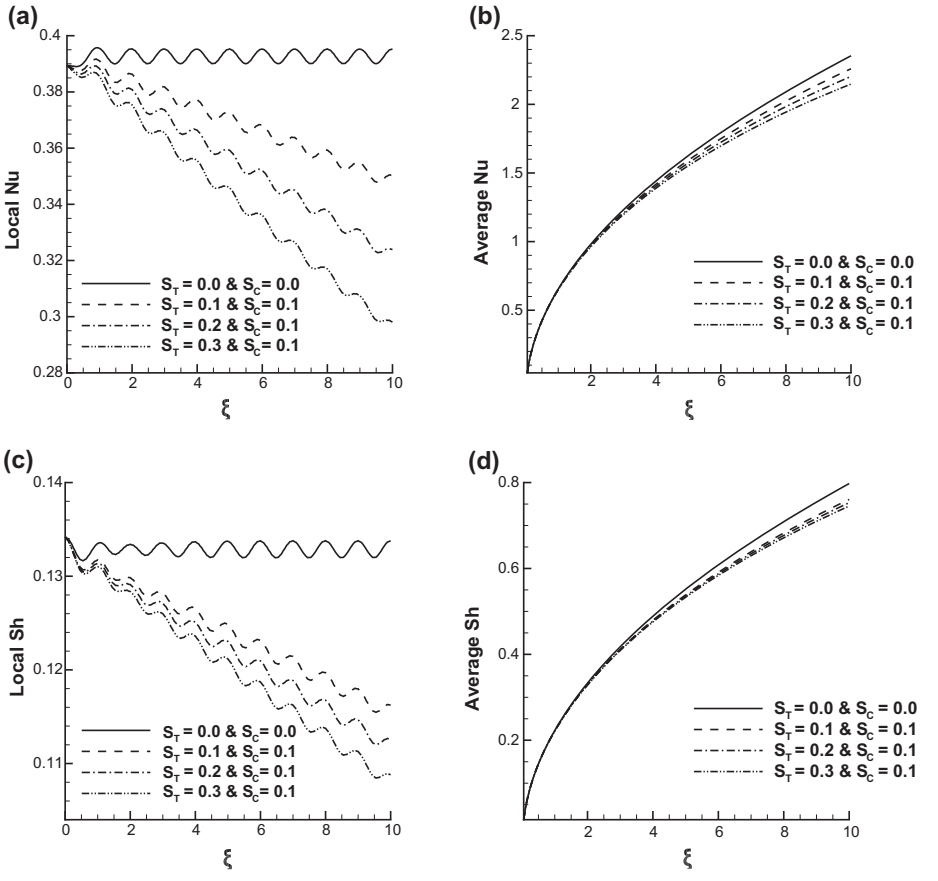

Figure 5. When fixing $a = 0.3$, $B = 1$, $Le = 1$, $M_g = 2$, $D_f = S_r = 0.025$ (a) Local Nu (b) Avg Nu (c) Local Sh (d) Avg Sh plots along the vertical wall for varying S_T.

of surface, while $S_T = S_C = 0$. Moreover, as the thermal (S_T) and mass (S_C) stratification parameters given some values, Local *Nu* and Local *Sh* curves get tilt from the horizontal direction in such manner that both Local *Nu* and Local *Sh* starts decreasing along the ξ axis. In addition to this, it is perceived that raising the thermal and mass stratification larger the tilt of Local *Nu* and Local *Sh* for the horizontal direction.

From the Figure 5(b), (d) it is observed given rise to the stratification parameters (S_C and S_T) decline the Average *Nu* and Average *Sh* levels. As a result of this, we can conclude that rising stratification increase the temperature and concentration gradients. Consequently, it boosts the free convective heat transfer all along the vertical surface and results into overall rise in temperature and concentration levels. Due to this behaviour of fluid flow, one can conclude that reduction in temperature and concentration gradients increase the thickness of thermal and concentration boundary layers. From the Figure 5(a)–(d), it is noticed that boundary layer thickness increases with rising in concentration coefficients.

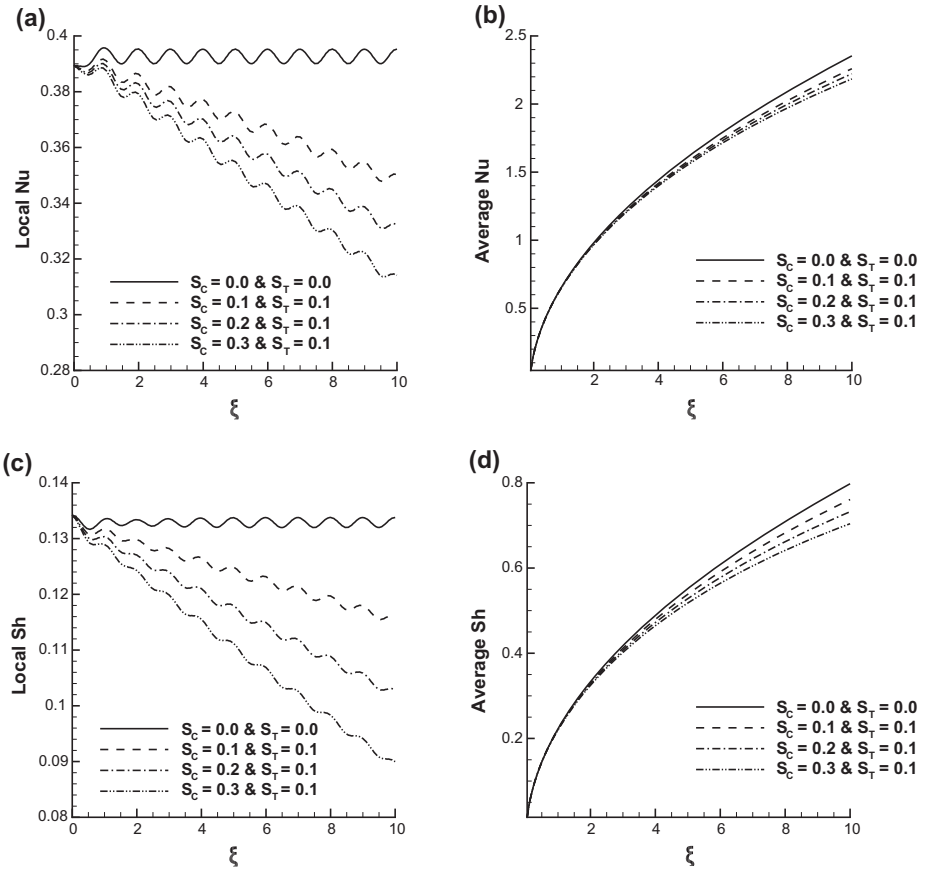

Figure 6. When fixing $a = 0.3$, $B = 1$, $Le = 1$, $M_g = 2$, $D_f = S_r = 0.025$ (a) Local Nu (b) Avg Nu (c) Local Sh (d) Avg Sh plots along the vertical wall for varying S_C.

4.4. Influence of Buoyancy ratio (B) on heat and mass transfer process

In Figure 8(a)–(d) Local Nu, Local Sh, Average Nu and Average Sh number plots have been analysed along the surface i.e $0 \leq \xi \leq 10$ for $B = -1, 0, 1, 2, 3, 4$, to investigate the impact of buoyancy ratio on heat and mass transfer process in doubly stratified MHD natural convection past a wavy vertical surface immersed in Darcy porous medium. Where other parameters have been fixes as $a = 0.3$, $M_g = 2$, $Le = 1$, $S_T = S_C = 0.025$, $D_f = S_r = 0.025$.

From Figure 8(a)–(d), one can notice that increasing the value of buoyancy ratio (B) is leading the increment in all the heat and mass flux parameters, i.e. Local Nu, Local Sh, Average Nu, Average Sh. In conclusion of such increment in Local Nu and Local Sh, it can be stated that raising the buoyancy (B) parameter enhance the heat and mass flux levels. From Figure 8(a), (c) It is observed that for small values of buoyancy ratio B, Local Nu is parallel to ξ axis or effect of stratification is noted insignificant. But rising B does retain such behaviour of Local Nu and Local Sh curves along ξ axis and the substantial amount of rise in

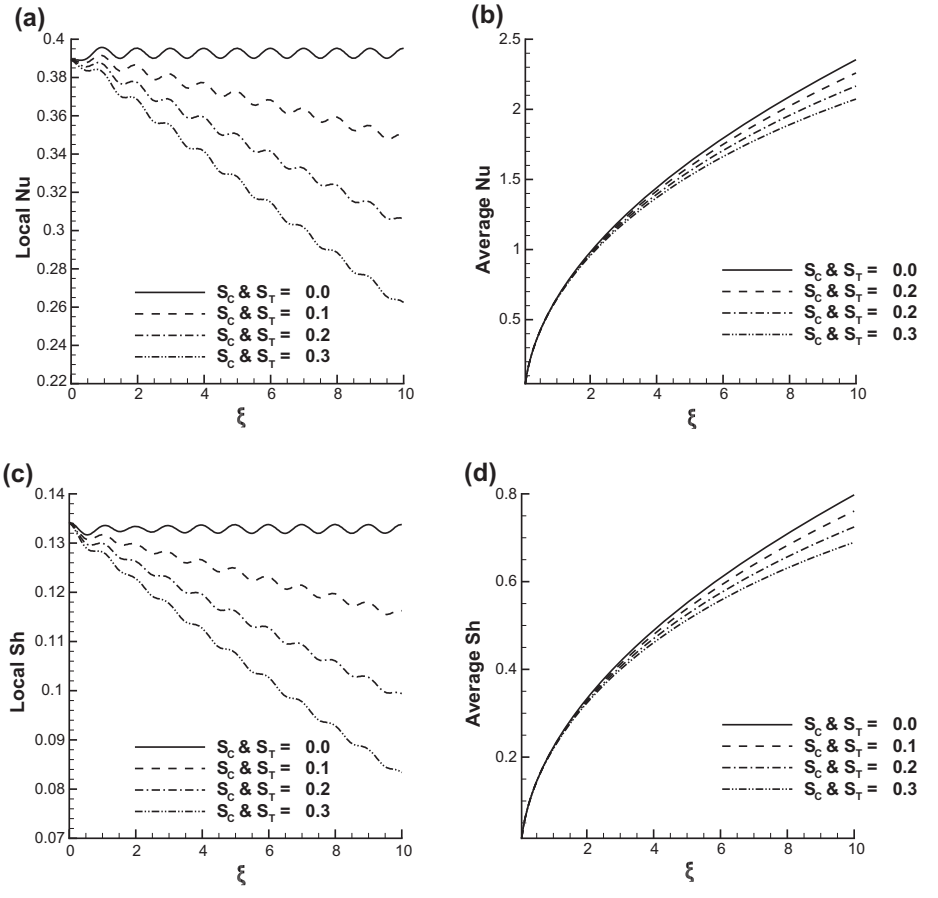

Figure 7. When fixing $a = 0.3$, $B = 1$, $Le = 1$, $M_g = 2$, $D_f = S_r = 0.025$ (a) Local Nu (b) Avg Nu (c) Local Sh (d) Avg Sh plots along the vertical wall for varying S_T and S_C.

influence due to both thermal and mass stratification is exhibited. From Figure 8(b), (d) it is perceived that raising the buoyancy ratio B make the sharp rise in Average *Nu* and Average *Sh* curves along the ξ axis. As the result of such finding one can remark that increasing slopes of Average *Nu* and Average *Sh* curves because of given rising in buoyancy ratio B diminish the thickness of boundary layer for both temperature and mass profile of fluid flow.

4.5. Influence of Lewis number (Le) on heat and mass transfer process

The influence of Lewis number on heat and mass transfer process near a vertical wavy surface immersed in doubly stratified fluid-saturated Darcy porous medium under the influence of MHD forces as well as Soret and Dufour effect have been analysed in 9(a)–(d) for $0 \leq Le \leq 1$ with having fixed $a = 0.3$, $M_g = 2$, $B = 2$, $S_T = S_C = 0.025$, $D_f = S_r = 0.025$.

From Figure 9(a), (c) it is perceived that raising the value of Lewis Number (Le) comes out with the drop in Local *Nu* and rise in Local *Sh*. On the other hand,

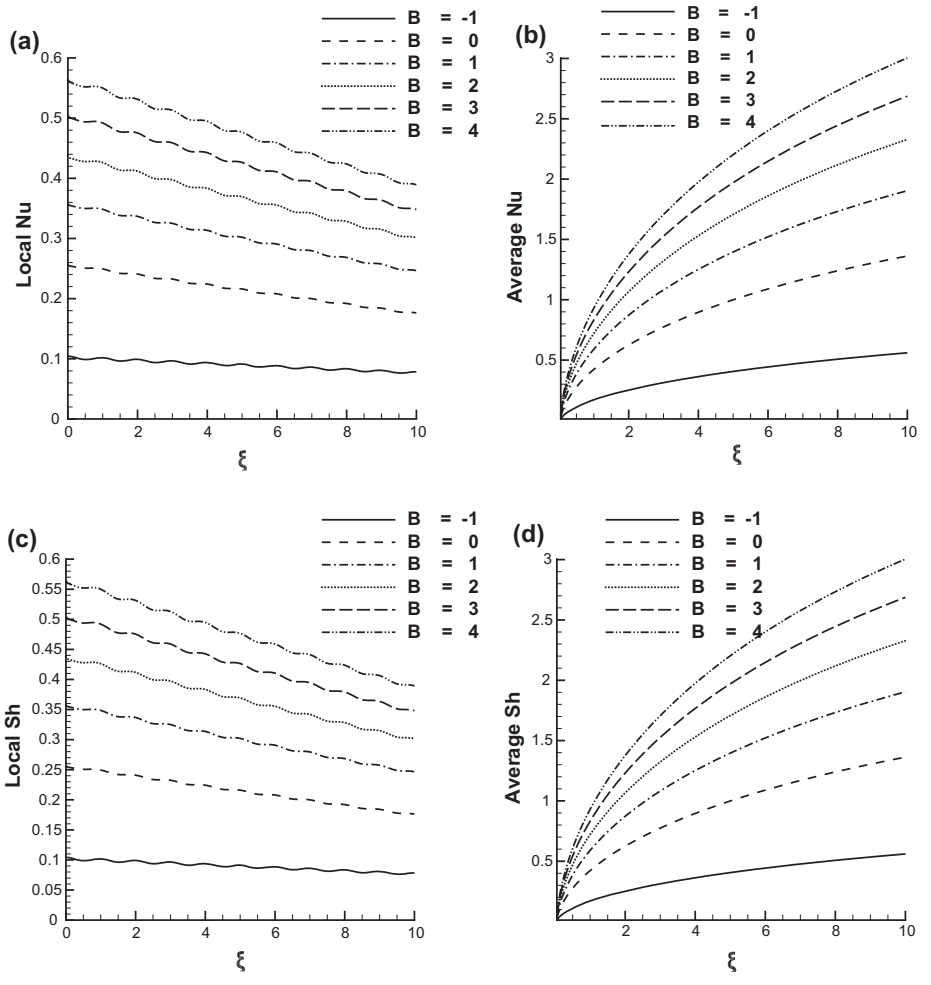

Figure 8. When fixing $a = 0.3$, $Le = 1$, $M_g = 2$, $S_r = D_f = 0.025$, $S_T = S_C = 0.025$ (a) Local Nu (b) Avg Nu (c) Local Sh (d) Avg Sh plots along the vertical wall for varying B.

the affect due to thermal stratification is straightforward with the rise in Le, whereas the impact of concentration stratification gets enhanced with growing values of Le. From Figure 9(b), (d), it is noticed that increasing the value of Lewis number (Le) brings fall in the Average Nu and hike in Average Sh. As a result of such behaviour, it can be stated that reduction in the thickness of concentration boundary layer makes thicker the thermal boundary layer due to growth in Le.

4.6. Influence of Soret (S_r) and Dufour (D_f) number on heat and mass transfer process

The influence of Dufour effect on heat and mass transfer process in double diffusive MHD free convection past a wavy vertical surface immersed in doubly stratified Darcy porous medium has been presented in Figure 10(a)–(d) for D_f =

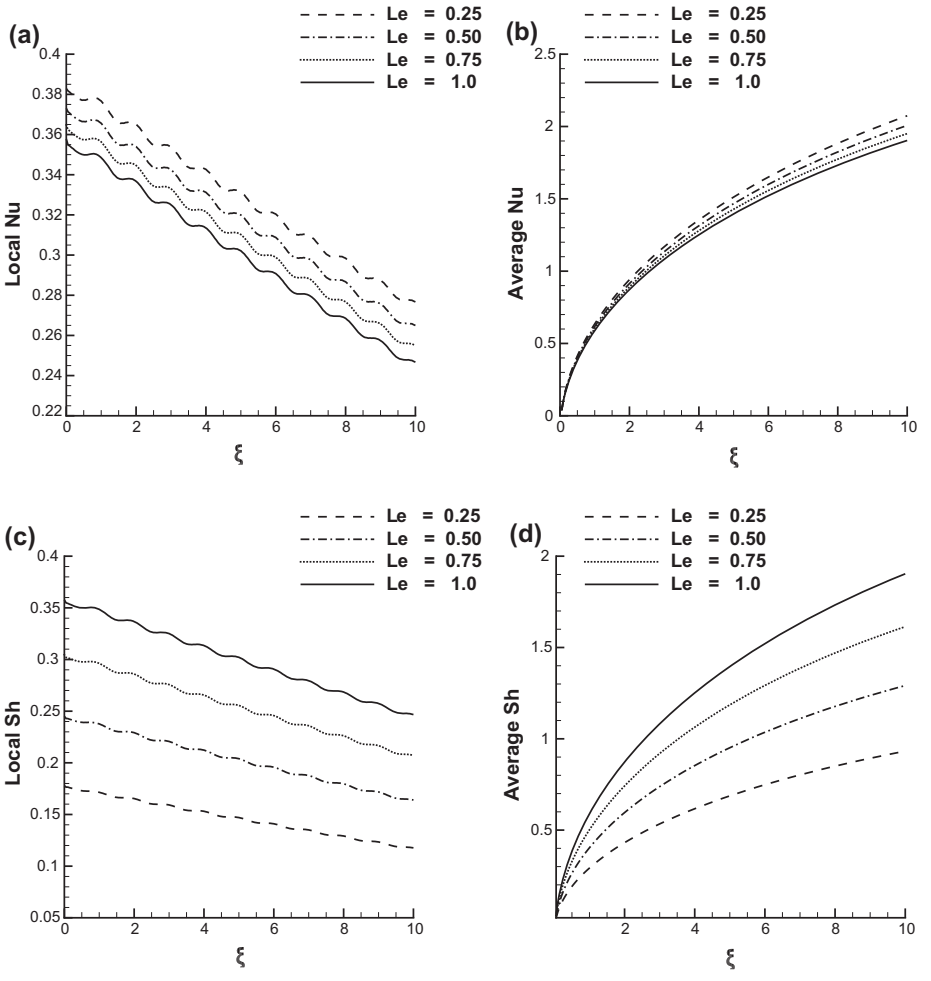

Figure 9. When fixing $a = 0.3$, $B = 2$, $M_g = 2$, $S_r = D_f = 0.025$, $S_T = S_C = 0.025$ (a) Local Nu (b) Avg Nu (c) Local Sh (d) Avg Sh plots along the vertical wall for varying *Le*.

0, 1, 2, 5, 10 together with having fixed $a = 0.3$, $M_g = 2$, $B = 1$, $Le = 0.1$, $S_T = S_C = 0.0125$, $S_r = 0.002$.

From the plots in Figure 10(a), (c), one can notice that due to raising the Dufour coefficient, Local *Nu* decreases, whereas Local *Sh* increases along the vertical surface. Consequently, it can be stated that the given rise in Dufour coefficient declines the thermal energy flux levels which cause the rise in overall temperature throughout the domain of flow. As a result of such growth in temperature profile leads towards the increment in concentration gradients. By the graphs in Figure 10(b), (d), it can be introduced that Average *Nu* decrease, while Average *Sh* increase due to rise in Dufour coefficient. In conclusion of such relative behaviour of Average *Nu* and Average *Sh*, one can remark that raising the temperature levels become the reason of increment in thickness of

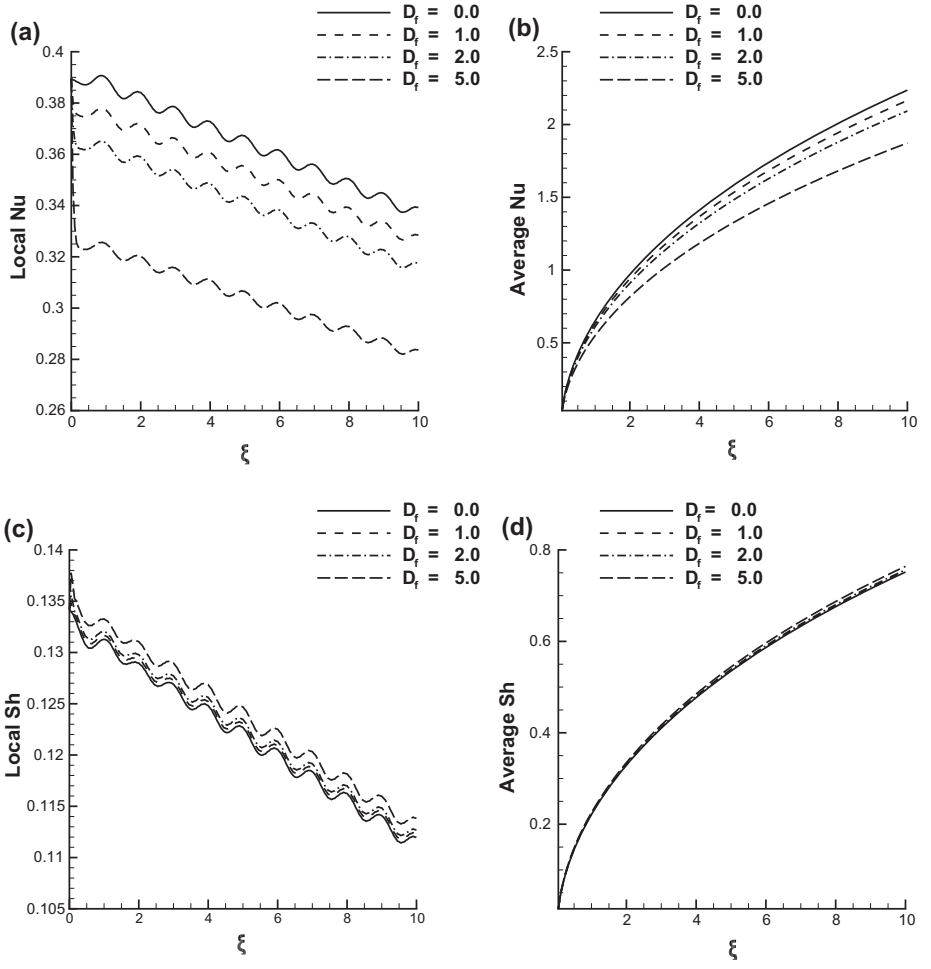

Figure 10. When fixing $a = 0.3$, $B = 1$, $Le = 0.1$, $M_g = 2$, $S_r = 0.002$, $S_T = S_C = 0.0125$ (a) Local Nu (b) Avg Nu (c) Local Sh (d) Avg Sh plots along the vertical wall for varying D_f.

the thermal boundary layer together with making the concentration boundary layer significantly thinner.

The impact of Soret effect on heat and mass transfer process in double diffusive MHD free convection past a wavy vertical surface immersed in doubly stratified Darcy porous medium has been analysed in Figure 11(a)–(d) for $0 \leq S_r \leq 10$ when fixing $a = 0.3$, $M_g = 2$, $B = 1$, $Le = 0.1$, $S_T = S_C = 0.0125$ and $D_f = 0.002$. From the plots in Figure 11(a), (c), one can notice that due to raising the Soret coefficient, Local *Nu* increases whereas Local *Sh* decreases along the vertical surface. Consequently, it can be stated that rise in Soret coefficient diminish the local mass flux levels which cause the rise in overall concentration of fluid throughout the domain of flow. As a result of such growth in concentration profile leads the increment in temperature gradients. From the graphs in Figure 10(b), (d), it can be introduced that Average *Nu* increases, while Average *Sh*

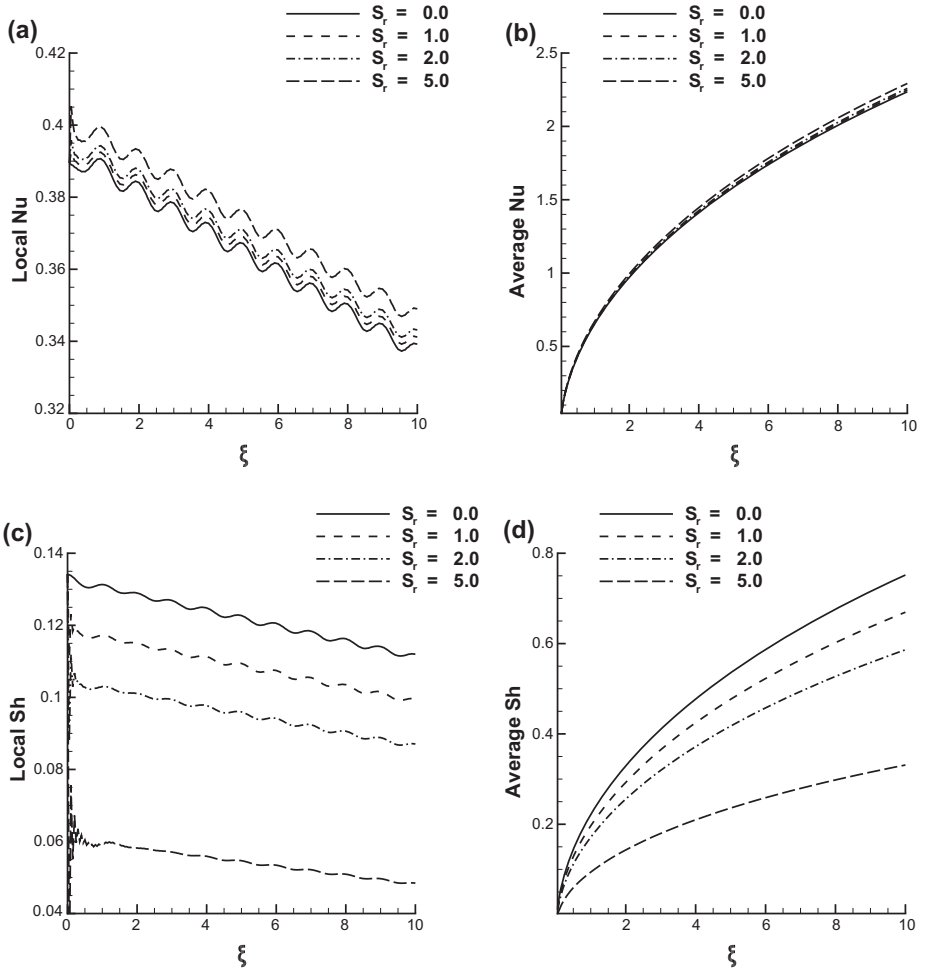

Figure 11. When fixing $a = 0.3$, $B = 1$, $Le = 0.1$, $M_g = 2$, $D_f = 0.002$, $S_T = S_C = 0.0125$ (a) Local Nu (b) Avg Nu (c) Local Sh (d) Avg Sh plots along the vertical wall for varying S_r.

decreases due to given rise in Soret coefficient. So that it is concluded that rising concentration levels become the reason to increase the thickness of the concentration boundary layer together with making the thermal boundary layer significantly thinner.

5. Conclusion

The combined effect of thermal and mass stratification together with Magnetohydrodynamic forces on double diffusive free convective heat and mass transfer past the vertical wavy surface immersed in Darcian fluid-saturated porous medium has been numerically investigated using Keller Box implicit finite difference scheme. Under these complex parameters of the fluid flow model, both heat and mass fluxes are found significantly influenced by the parameters amplitude of wavy surface (a), magnetohydrodynamic forces (M_g), thermal and mass

stratification (S_T, S_C), Lewis number (Le), Buoyancy ratio (B), Soret (S_r) and Dufour (D_f) numbers. While increasing values of amplitude of wavy surface, thermal or mass stratification, MHD forces, Lewis number and Dufour effect results in the drop of LHTFLXs, whereas the rise in buoyancy ratio and Soret effect parameter favours the increment in LHTFLXs. On the other hand, raising the magnitudes of the amplitude of wavy surface, Thermal or Mass stratification, MHD forces, Soret number make fall in LMFLXs and increment of Dufour effect, buoyancy ratio and Lewis number uplift LMFLXs.

The study of thermally stratified systems in fluid flow through porous media has many applications like: geothermal, solar and biomass as well as for waste heat recovery from power plants and industrial processes, etc. The thermally stratified design will contain the renewable and sustainable energy technology and this technology has the capability to supply the required amount of high as well as low-temperature energy at various power extents and time-steps. In order to robust the design, there is a need to establish the control on acquired power levels. As per the observations by introducing the wavy surface, it boosts the temperature and concentration profile of fluid flow. Moreover, when the magnetic forces are applied transversally to the vertical surface which is maintained at uniform temperature and concentration it leads to the resistance to the horizontal velocity components. It is essential to study the thermal and mass stratification under the MHD forces along the wavy surface for the well-controlled design of thermal storage tanks. So that present study may be helpful in designing the thermally stratified systems of thermal storage tanks.

Disclosure statement

No potential conflict of interest was reported by the authors.

References

Boerner, C. J., Quack, H., & Sparrow, E. M. (1970). Local nonsimilarity boundary-layer solutions. *AIAA Journal, 8*(11), 1936–1942.

Bejan, A., & Khair, K. R. (1985). Heat and mass transfer by natural convection in a porous medium. *International Journal of Heat and Mass Transfer, 28*(5), 909–918.

Cheng, C.-Y. (2000). Natural convection heat and mass transfer near a vertical wavy surface with constant wall temperature and concentration in a porous medium. *International Communications in Heat and Mass Transfer, 27*(8), 1143–1154.

Cheng, C.-Y. (2009). Combined heat and mass transfer in natural convection flow from a vertical wavy surface in a power-law fluid saturated porous medium with thermal and mass stratification. *International Communications in Heat and Mass Transfer, 36*(4), 351–356.

Elgazery, N. S., & Elazem, N. Y. A. (2009). The effects of variable properties on MHD unsteady natural convection heat and mass transfer over a vertical wavy surface. *Meccanica, 44*(5), 573–586.

Ergun, S. (1952). Fluid flow through packed columns. *Chemical Engineering Progress, 48*, 89–94.

Geindreau, C., & Auriault, J.-L. (2002). Magnetohydrodynamic flows in porous media. *Journal of Fluid Mechanics, 466*, 343–363.

Gorla, R. S. R., & Chamkha, A. (2011). Natural convective boundary layer flow over a nonisothermal vertical plate embedded in a porous medium saturated with a nanofluid. *Nanoscale and Microscale Thermophysical Engineering, 15*(2), 81–94.

Hady, F. M., Mohamed, R. A., & Mahdy, A. (2006). MHD free convection flow along a vertical wavy surface with heat generation or absorption effect. *International Communications in Heat and Mass Transfer, 33*(10), 1253–1263.

Ingham, D. B., & Pop, I. (2005). *Transport phenomena in porous media* (Vol. 3). Oxford: Elsevier. ISBN 9780080444901,0-0804-4490-3.

Isaacson, E., & Keller, H. B. (1994). *Analysis of numerical methods*. New York, NY: Courier Corporation.

Kabir, K. H., Alim, M. A., & Andallah, L. S. (2013). Effects of viscous dissipation on MHD natural convection flow along a vertical wavy surface with heat generation. *American Journal of Computational Mathematics, 3*(02), 91–98.

Keller, H. B., & Cebeci, T. (1971). *Lecture notes in physics* (Vol. 8, pp. 91–100). New York, NY: Springer Verlag.

Kumar, B. V. R., & Shalini (2004). Double-diffusive natural convection induced by a wavy surface in a stratified porous medium. *Journal of Porous Media, 7*(4). ISSN 1091-028X.

Mahdy, A. (2009). MHD non-darcian free convection from a vertical wavy surface embedded in porous media in the presence of Soret and Dufour effect. *International Communications in Heat and Mass Transfer, 36*(10), 1067–1074.

Molla, Md. M., Hossain, Md. A., & Yao, L. S. (2004). Natural convection flow along a vertical wavy surface with uniform surface temperature in presence of heat generation/absorption. *International Journal of Thermal Sciences, 43*(2), 157–163.

Narayana, P. A. L., & Sibanda, P. (2010). Soret and Dufour effects on free convection along a vertical wavy surface in a fluid saturated darcy porous medium. *International Journal of Heat and Mass Transfer, 53*(15), 3030–3034.

Nield, D. A., & Bejan, A. (2006). *Convection in porous media*. New York, NY: Springer Science & Business Media.

Postelnicu, A. (2004). Influence of a magnetic field on heat and mass transfer by natural convection from vertical surfaces in porous media considering Soret and Dufour effects. *International Journal of Heat and Mass Transfer, 47*(6), 1467–1472.

Roussellet, V., Niu, X., Yamaguchi, H., & Magoulés, F. (2011). Natural convection of temperature-sensitive magnetic fluids in porous media. *Advances in Applied Mathematics and Mechanics, 3*(01), 121–130.

Rees, D. A. S., & Pop, I. (1994). A note on free convection along a vertical wavy surface in a porous medium. *Journal of Heat Transfer, 116*(2), 505–508.

Rees, D. A. S., & Pop, I. (1997). The effect of longitudinal surface waves on free convection from vertical surfaces in porous media. *International Communications in Heat and Mass Transfer, 24*(3), 419–425.

Tak, S. S. & Lodha, A. (2007). Influence of double stratification on MHD free convection with Soret and Dufour effects in a darcian porous media. *PAMM, 7*(1), 2100089–2100090.

Takhar, H. S., & Ram, P. C. (1994). Magnetohydrodynamic free convection flow of water at 4 c through a porous medium. *International Communications in Heat and Mass Transfer, 21*(3), 371–376.

Tashtoush, B., & Al-Odat, M. (2004). Magnetic field effect on heat and fluid flow over a wavy surface with a variable heat flux. *Journal of Magnetism and Magnetic Materials, 268*(3), 357–363.

Tsai, R., & Huang, J. S. (2009). Numerical study of Soret and Dufour effects on heat and mass transfer from natural convection flow over a vertical porous medium with variable wall heat fluxes. *Computational Materials Science, 47*(1), 23–30.

Vafai, K. (2015). *Handbook of porous media* (3rd ed.). New York, NY: CRC Press. ISBN 978-1-4398-8557-4,1439885575.

Vafai, K., & Hadim, H. (2000). Natural and mixed convection. *Advances in Numerical Heat Transfer, 2*, 331–371.

Yu, H. S., & Sparrow, E. M. (1971). Local nonsimilarity thermal boundary layer solutions. *ASME Journal of Heat Transfer, 93*, 328–334.